GPS L5 and GALILEO E5a/E5b signal-to-noise density ratio degradation due to DME/TACAN signals : simulations and theoretical derivation

Frédéric Bastide, Eric Chatre, Christophe Macabiau, Benoit Roturier

GPS L5 and GALILEO E5a/E5b Signal-to-Noise Density Ratio Degradation due to DME/TACAN Signals: Simulations and Theoretical Derivation

Frederic Bastide, ENAC/STNA, France
Eric Chatre, Galileo Interim Support Structure, France
Christophe Macabiau, ENAC, France
Benoit Roturier, STNA, France

BIOGRAPHIES

Frederic Bastide graduated as an electronics engineers at the ENAC, the French university of civil aviation, in 2001, Toulouse. He is now a Ph.D student at the ENAC. Currently he is working on DME/TACAN and JTIDS/MIDS signals impact on GNSS receivers. He also spent 6 months at the Stanford GPS Lab in 2003 as an exchange researcher.

Eric Chatre graduated as an electronics engineer in 1992 from the ENAC (Ecole Nationale de l'Aviation Civile), Toulouse, France. From 1994 to 2001, he worked with the Service Technique de la Navigation Aérienne (STNA) in Toulouse on implementation of satellite navigation in civil aviation. He is now part of the Galileo Interim Support Structure where he is in charge of standardisation and certification matters. He is secretary of Eurocae WG 62.

Christophe Macabiau graduated as an electronics engineer in 1992 from the ENAC (Ecole Nationale de l'Aviation Civile) in Toulouse, France. Since 1994, he has been working on the application of satellite navigation techniques to civil aviation. He received his Ph.D. in 1997 and has been in charge of the signal processing lab of the ENAC since 2000.

Benoit Roturier graduated as a CNS systems engineer from Ecole Nationale de l'Aviation Civile (ENAC), Toulouse in 1985 and obtained a PhD in Electronics from Institut National Polytechnique de Toulouse in 1995. He was successively in charge of Instrument Landing Systems at DGAC/STNA (Service Technique de la Navigation Aerienne), then of research activities on CNS systems at ENAC. He is now head of GNSS Navigation subdivision at STNA and is involved in the development of civil aviation applications based on GPS/ABAS, EGNOS and Galileo.

ABSTRACT

In the coming years, additional radio navigation signals will be broadcast. For the civil aviation community, the GPS L5 signal and GALILEO E5a and E5b signals are of particular interest. Indeed they will be broadcast in an ARNS band and are expected to increase accuracy, availability, integrity and continuity of service. However E5a/L5 and E5b bands interfering environment is heavy and has been presented in several papers. In particular, Distance Measuring Equipment (DME) and Tactical Air Navigation (TACAN) systems operate in the 960-1215 MHz frequency band also allocated to these new GNSS signals. These pulsed navigation systems consist of an airborne interrogator and a ground-based transponder that emits high-power signals constituting a real threat.

The aim of this paper is to propose a new assessment of the impact of such interference on future GNSS receivers. This impact is evaluated through the computation of the equivalent post-correlation signal-to-noise density ratio degradation. Degradation is derived from the Signal-to-Noise plus Interfererence ratio (SNIR) at the prompt correlator output. Obtained results are useful to assess performance of receiver functions using prompt correlator sums such as signal acquisition and carrier phase tracking. DME/TACAN degradations have already been assessed by other authors but we bring here more accurate software and theoretical tools and the corresponding results. Degradation computation is carried out in two different ways. First, a realistic receiver simulator is used that processes useful GNSS signals and interfering DME/TACAN signals. Then, a theoretical derivation of degradation has been developed taking into account separately the effects of low-level and high-level pulses. One important assumption for interference generation is that arrival times of pulses follow a Poisson distribution that is used to assess the effect of pulse collisions. Another important aspect of the theoretical analysis is the consideration of the interference carrier effect yielding low blanker duty cycles but contributing to the

degradation. Results obtained with the two methods are compared for a worst case scenario at high altitude (FL 400) with and without safety margins over Europe.

INTRODUCTION

E5a/L5 and E5b bands interfering environment is presented in [1,2]. It is highlighted that major existing interfering systems are pulsed and that the main threat is DME/TACAN signals. There are pulse-ranging navigation systems operating in the 960-1215 MHz frequency band. DME signal provides distance measurement between the aircraft and a ground station. TACAN also provides azimuth information and is a military system. These navigation systems consist of an airborne interrogator and a ground-based transponder. DME/TACAN operate in four modes (X, Y, W and Z) and only the X-mode replies in the 1151-1213 MHz frequency band. X-mode replies are made of pulse pairs with an inter-pulse interval of 12 μs.

In the first part of this paper, the selected generic receiver model considered for theoretical derivation and simulations is presented. This model includes the front-end equivalent filters (directly driven by the currently proposed EUROCAE and RTCA interference masks), the Automatic Gain Control (AGC) and the ADC that are carefully designed to work in a pulsed environment by implementing digital pulse blanking. Then useful GNSS signals and interference signal modelizations are indicated along with the statistical approach implemented to generate DME/TACAN pulse pairs arrival times.

Then, a theoretical study of the equivalent post-correlation C/N_0 degradation resulting from these interfering signals is detailed. Theoretical degradations are also computed over the whole of Europe and geographical maps are presented to highlight the topography of these degradations. The paper further describes the realistic single-channel E5a/L5 and E5b receiver simulator used to run simulations. Since GPS L5 and GALILEO E5a signal structures will be identical, we assumed degradations brought by DME/TACAN are the same for these two signals. GALILEO E5b signal structure will also be identical; the sole difference lies in the equivalent RF/IF filter. Results obtained by the two approaches are indicated and compared over Europe for multiple safety margins. Finally, analyses were conducted to determine the optimal blanking threshold and degradation sensibility to beacon reallocation.

GENERIC RECEIVER SCHEME

Equivalent post-correlation C/N_0 degradation is computed from prompt inphase correlator output samples. A basic correlator is illustrated below in the receiver scheme. The received signal $s_R(t)$ at the antenna port is first filtered by the equivalent RF/IF front-end filter $H(f)$. The filtered signal $s_f(t)$ is multiplied by the Automatic Gain Control (AGC) gain and is sampled/quantized by the Analog-to-Digital Converter (ADC). Digital pulse blanking is implemented within the ADC so as to cope with pulsed interference. Digital samples are then multiplied by the local carrier and code replica. Finally, the resulting signal is integrated over N samples.

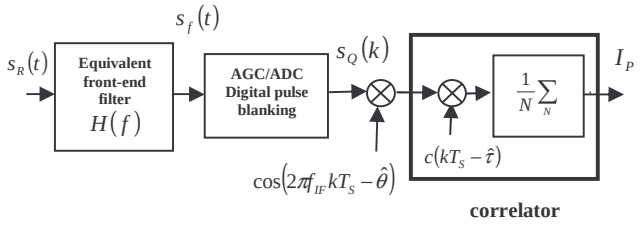

Figure 1 *Single channel receiver front-end and correlator*

In the previous figure,

- f_{IF} is the final intermediate frequency
- $\hat{\theta}$ is the tracked GNSS signal carrier phase estimate
- $c(t)$ is either le data ($c_{XI}(t)$) or pilot ($c_{XQ}(t)$) local code replica
- $\hat{\tau}$ is the tracked GNSS signal code delay estimate
- T_S is the sampling period
- N is the number of samples so that $N.T_S$ equals the coherent integration time T_P

As a basis, we considered two different out-of-band filtering requirements at L5/E5a. The first one was proposed by RTCA [1] and the other one by EUROCAE [3]. Then we sought to simulate filters as close as possible to the masks to assess the influence of the mask selection on degradation. Of course the obtained degradations will constitute a worst case since real-world filtering will be more stringent especially in stop-bands. Both requirements and simulated filters are shown on Figure 2. For the two filters, pass-band is [E5a-10 MHz,E5a+10 MHz]. On E5b, an interference mask has also been proposed by EUROCAE [3] and a corresponding front-end filter was simulated as shown on Figure 3. In this case, pass-band is [E5b-10 MHz,E5b+4 MHz].

The equivalent RF/IF filter is simulated as a succession of a IIR Butterworth filter and a FIR filter. Steep slope in the stop-band is achieved by a FIR filter that simulates IF filters effects. Lower slope away from the pass-band is brought by the Buterworth filter as RF filters do in real receivers.

The AGC is a variable gain amplifier whose role is to adapt its gain to reduce quantization losses. Given the front-end filter bandwidth and the number of bits there is an optimal gain [4,5]. The AGC system can be analog or digital by, for instance, looking at ADC bins distribution.

The system selected to cope with DME/TACAN signals is a digital blanker implemented within the ADC [6]. Samples are zeroed on a sample-by-sample basis: each individual quantized sample whose absolute value is above the blanking threshold is zeroed. Because there is a limited number of possible blanking thresholds (i.e. 2^{n-1} with n the number of bits), this digital implementation implies blanking threshold quantization as well. The blanker is characterized by its characteristic function χ_{blank} equal to 0, in case of signal suppression, otherwise to 1. Moreover, blanked samples shouldn't be used to drive the AGC gain to avoid incorrect gain adaptation due to interference.

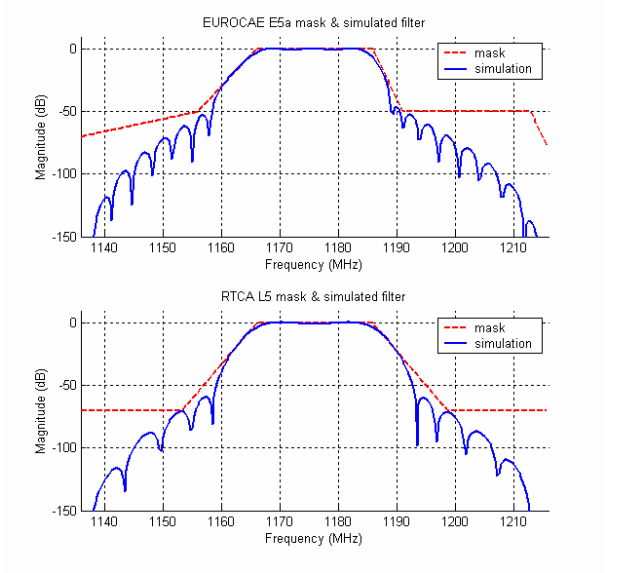

Figure 2 *RTCA and EUROCAE interference masks and simulated filters on E5a/L5 bands*

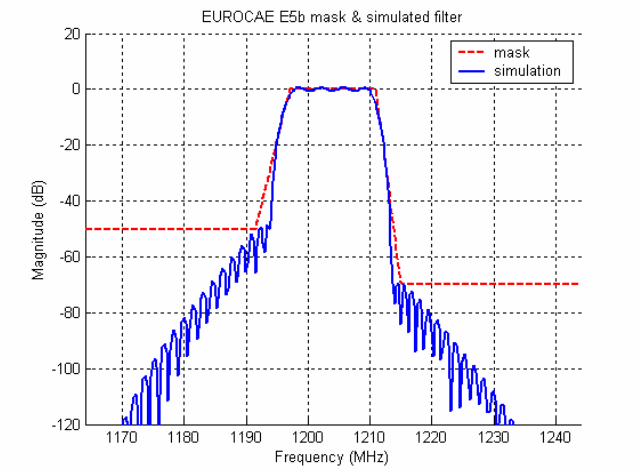

Figure 3 *EUROCAE interference masks and simulated filter on E5b*

SIGNALS EXPRESSIONS

The composite filtered signal $s_f(t)$ is the sum of the filtered useful tracked GNSS signal $s_{GNSS,f}(t)$, filtered receiver thermal noise $n_f(t)$ plus filtered DME/TACAN signals $s_{jammer,f}(t)$. Note that other received GNSS signals that would cause inter-system or inter-system interference are neglected.

The useful considered GNSS signals within E5a/L5 and E5b bands are QPSK modulations. There are assumed composed of two equal-power signal components: the data component, carrying data, and the pilot component without any data. For instance details about the GPS L5 signal may be found in [7] and information on future GALILEO signals in [8]. After down-conversion and front-end filtering they may be expressed as

$$\begin{aligned} s_{GNSS,f}(t) = \sqrt{P_{GNSS}}.d(t-\tau).c_{XI,f}(t-\tau) \\ .NH_{10}(t-\tau).\cos(2\pi f_{IF}t-\theta) \\ +\sqrt{P_{GNSS}}.c_{XQ,f}(t-\tau).NH_{20}(t-\tau) \\ .\sin(2\pi f_{IF}t-\theta) \end{aligned}$$

where

- P_{GNSS} is the total (data+pilot) received power at the antenna port
- $d(t)$ is the P/NRZ/L materialization of the navigation message
- $c_{XI,f}$ and $c_{XQ,f}$ are respectively the filtered PRN codes used on the data and pilot components
- *NH10* and *NH20* are respectively the P/NRZ/L materialization of the Neuman-Hoffman codes used on the data and pilot components
- τ is time-varying received signal code delay
- θ is time-varying received signal carrier phase

Receiver thermal noise is modelized as a zero-mean Gaussian white noise whose PSD equates $N_0/2$. The filtered noise $n_f(t)$ is zero-mean and its PSD is simply $N_0/2.|H(f)|^2$.

Concerning DME/TACAN signals, each signal may be modelized as a succession of Gaussian-shape pulse pairs, each pulse having a 3.5 µs half-amplitude duration. A pulse pair has the following expression and is illustrated in the Figure 4 [9].

$$s_{pulse\ pair}(t) = e^{-\frac{\alpha}{2}t^2} + e^{-\frac{\alpha}{2}(t-\Delta t)^2}$$

where

- α =4.5e11 s^{-2}
- Δt =12e-6 s is the inter-pulse interval

In the theoretical derivation, filtering impact is only accounted for on the received interfering power and not on the possible pulse shape deformation. This is true when the interfering signal frequency is located over flat frequency response regions (i.e. pass-band). Elsewhere (i.e. stop-band) it is not rigorously true. Thus the down-converted and filtered DME/TACAN signal expression is

$$s_{DME/TACAN,f}(t) = \sqrt{J.|H(f_J)|^2} \sum_k \left(e^{\frac{-\alpha(t-t_k)^2}{2}} + e^{\frac{-\alpha(t-\Delta t-t_k)^2}{2}} \right) \cos\left(2\pi\left(f_{IF} + \Delta f_{jammer}\right)t + \theta_J\right)$$

where

- J is the jammer peak power at the antenna port
- f_J is the received jammer carrier frequency
- $\{t_k\}$ is the ensemble of pulse pairs arrival times
- Δ_{jammer} is the frequency offset of the jammer carrier with respect to either E5a/L5 or E5b
- θ_J is the jammer carrier phase

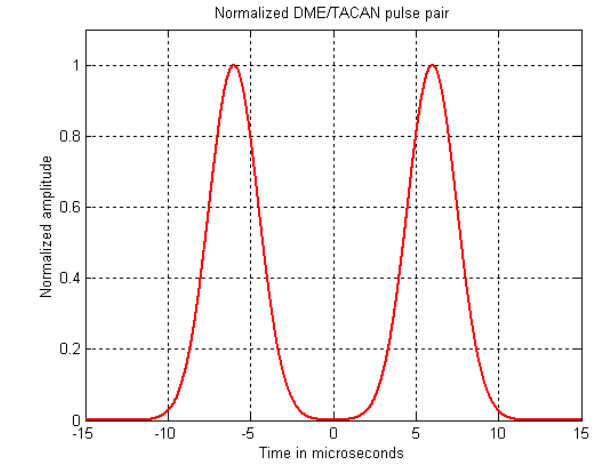

Figure 4 *Normalized DME/TACAN pulse pair*

We assumed ground stations transmit pairs at a maximum rate (pulse repetition frequency - PRF) of 2700 ppps (pulse pairs per second) for DMEs and 3600 ppps for TACANs. This figure represents the mean number of pairs per second. Arrival times of pair pulses are random and may be assumed independent and of constant behavior over time for each ground beacon. Thus a convenient modelization is a Poisson distribution with parameter λ equal to the PRF. An illustration of such generated DME signal, modulating a carrier, is given on Figure 5 over 2 ms. On average, there should be 5.4 pulse pairs over 2 ms, in this snap-shot only 4 pairs appear.

In some previous analysis, i.e. [9], DME/TACAN signals were assumed periodical and without any pulse pairs collisions. This modelization was not realistic but our model enables collisions as shown on Figure 6. The plotted composite DME/TACAN interfering signal is simply the sum over the whole beacon ensemble of the previous generic jammer signal expression $s_{DME/TACAN,f}(t)$.

Carrier phases of signals are random and may be assumed uniformly distributed over [0,2π[so each jammer is centered and so is the sum.

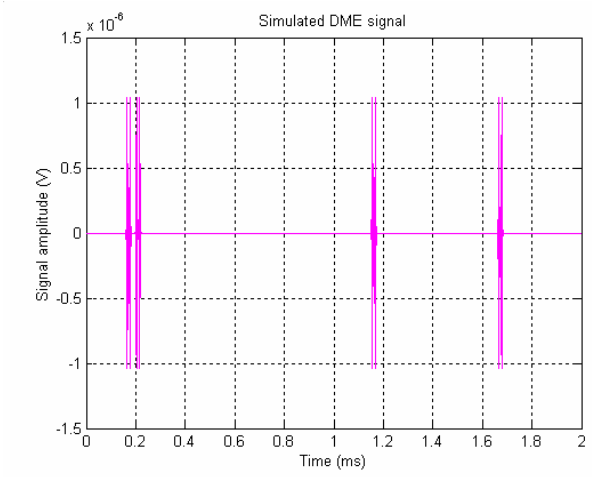

Figure 5 *Simulated DME signal over 2 ms*

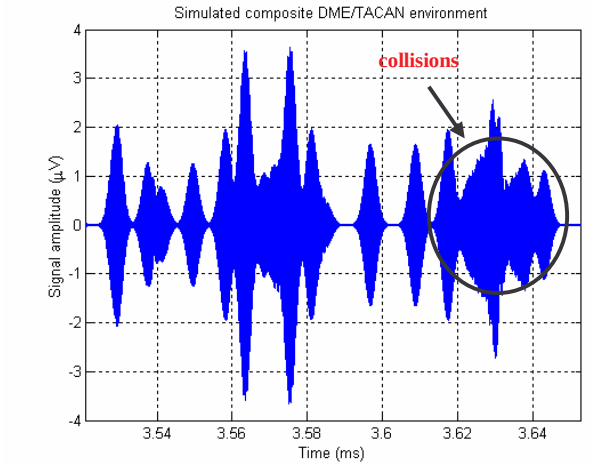

Figure 6 *Example of composite DME/TACAN signals environment*

The filtered signals are then multiplied by the AGC gain G_{AGC} and sampled/quantized by the ADC yielding

$$s_Q(k) = G_{AGC}.s_f(k) + e_Q(k)$$

where e_Q is the quantization error. This error is assumed uncorrelated from the input signal thus quantization losses may be accounted for separately from degradations due to interfering signals. The power link budget will group them. **The AGC/ADC systems and associated losses being not addressed in this paper, theoretical derivation and simulations do not consider these processes. As a consequence signal expressions and mathematical calculus are carried out using continuous-time signals.**

Finally, the data or pilot prompt inphase correlator output is the sum of contributions of each signal:

$$I_P = I_{GNSS,P} + I_{n,P} + \sum_i I_{jammer,P,i}$$

The summation is over all the received DME/TACAN beacon signals.

EQUIVALENT POST-CORRELATION SIGNAL-TO-NOISE DENSITY RATIO DEGRADATION

This degradation may be calculated from either the data or pilot prompt correlator output Signal-to-Noise plus interference Ratio (SNIR) degradation. We chose to consider the pilot component for the theoretical derivation. The classical definition of the SNIR is the ratio of the squared mean of the prompt correlator output divided by its variance [10]:

$$SNIR = \frac{E[I_P]^2}{Var[I_P]}$$

The numerator of this ratio equates the useful signal power available while the denominator is the noise plus interference power. First, the theoretical methodology developed to assess this degradation is presented. Then the realistic GNSS receiver simulator also used to carry out degradation estimation is presented.

Useful signal power degradation at correlator output

In this section the useful power available at correlator output is expressed when a digital blanker is implemented. This power is $E[I_P]^2 = E[I_{GNSS,P}]^2$ given that both thermal noise and DME/TACAN signals are zero-mean. Neglecting double-frequency terms that are filtered by the I&D filter and the data/pilot spreading codes cross-correlation, the GNSS pilot prompt correlator output signal $I_{GNSS,P}$ is

$$I_{GNSS,P} = \frac{G_{AGC}}{2.T_P}.\int_{T_P} \sqrt{P_{GNSS}}.c_{XQ,f}(t-\tau).c_{XQ}(t-\hat{\tau}).\cos(\theta-\hat{\theta}).\chi_{blank}(t).dt$$

The blanking function may be assumed independent from both the useful GNSS signal and thermal. Indeed, this function mainly depends on pulsed interference which are the predominant signals. So,

$$E[I_{GNSS,P}] = \frac{\sqrt{P_{GNSS}}.G_{AGC}}{2.T_P}.\int_{T_P} .E[c_{XQ,f}(t-\tau).c_{XQ}(t-\hat{\tau})]E[\cos(\theta-\hat{\theta})]E[\chi_{blank}(t)].dt$$

Suppose in the following code and carrier phases tracking processes are perfect so that $\tau = \hat{\tau}$ and $\theta = \hat{\theta}$. Then, previous expression leads to

$$E[I_{GNSS,P}]^2 = \frac{G_{AGC}^2.P_{GNSS}.K_{c,f}^2(0)}{4.T_P^2}.[T_P.E[\chi_{blank}]]^2$$

where $K_{c,f}(\tau)=E[c(t)c_f(t-\tau)]$ is the cross-correlation between the spreading code and its filtered version. The expected value of the blanking function equates

$$E[\chi_{blank}] = 1 - Bdc$$

Where, by definition, *Bdc* is called the blanker duty cycle. It is expressed as the ratio of the portion of time $T_{blanker}$ where the blanker is "on" (signal set to zero) to the coherent integration time: $Bdc=T_{blanker}/T_P$.

Let denote $\alpha=K_{c,f}^2(0)$, α refers to as the useful signal power loss at correlator output due to front-end filtering. The useful signal power at correlator output is then

$$E[I_{GNSS,P}]^2 = \alpha.\frac{G_{AGC}^2.P_{GNSS}}{4}.(1-Bdc)^2$$

In the absence of blanker it becomes

$$E[I_{GNSS,P}]^2 = \alpha.\frac{G_{AGC}^2.P_{GNSS}}{4}$$

So the useful signal power degradation $\deg(signal)$ is

$$\boxed{\deg(signal) = (1-Bdc)^2}$$

Noise floor adjustment

The global noise at correlator output comes from both thermal noise and DME/TACAN signals contributions and has the following expression

$$\begin{aligned} Var[I_P] &= E[(I_P - E(I_P))^2] = E[(I_P - I_{GNSS,P})^2] \\ &= E[(I_{n,P} + I_{jammer,P})^2] \\ &= E[I_{n,P}{}^2] + 2E[I_{n,P}.I_{jammer,P}] + E[I_{jammer,P}{}^2] \end{aligned}$$

Each of these terms is expressed below

1. **the first one corresponds to the receiver thermal noise contribution**

$$\begin{aligned} E[I_{n,P}^2] &= E\left[\left(\frac{G_{AGC}}{T_P}\int_{T_P} n(t)c(t-\hat{\tau})\cos(2\pi f_{IF}t-\hat{\theta})\chi_{blank}(t).dt\right)^2\right] \\ &= \frac{G_{AGC}^2}{T_P^2}E\left[\int_{T_P}\int_{T_P} n(t)n(u)c(t-\hat{\tau})c(u-\hat{\tau})\cos(2\pi f_{IF}t-\hat{\theta})\cos(2\pi f_{IF}u-\hat{\theta})\chi_{blank}(t)\chi_{blank}(u).dt.du\right] \\ &= \frac{G_{AGC}^2}{T_P^2}\int_{T_P}\int_{T_P} K_n(t-u)K_C(t-u)E(\cos(2\pi f_{IF}t-\hat{\theta})\cos(2\pi f_{IF}u-\hat{\theta}))E(\chi_{blank}(t)\chi_{blank}(u)).dt.du \end{aligned}$$

Front-end filtering is neglected for the moment thus thermal noise is supposed white and its autocorrelation function is $K_n(\tau)=N_0/2.\delta(\tau)$ so the double integral is non null only when $t=u$. Thus,

$$E\left[I_{n,P}^2\right]=\frac{G_{AGC}^2}{T_P^2}.\frac{N_0}{2}.K_C(0).\frac{1}{2}.K_{\chi_{blank}}(0).T_P$$

The blanking function autocorrelation is denoted $K_{\chi\,blank}(\tau)$ whose value in 0 is equal to the blanking function power expressed below,

$$K_{\chi_{blank}}(0)=E\left(\chi_{blank}^2\right)=\Pr\left(\chi_{blank}=1\right)=1-Bdc$$

Finally, the correlator output power due to thermal noise is

$$E\left[I_{n,P}^2\right]=\frac{G_{AGC}^2.N_O.f_P}{4}.(1-Bdc)$$

Without blanker, the power is

$$E\left[I_{n,P}^2\right]=\frac{G_{AGC}^2.N_O.f_P}{4}$$

So eventually, the thermal noise power degradation *deg(thermal noise)* expression is

$$\boxed{\deg(thermal\ noise)=(1-Bdc)}$$

Note:

Because of the front-end filtering, output power is lower, indeed it can be shown [11] that

$$E\left[I_{n,P}^2\right]=\beta.G_{AGC}^2.\frac{N_0.f_P}{4}.(1-Bdc)$$

with $\beta=\int_{-\infty}^{+\infty}S_c\left(f-\Delta f_{assym}\right).\left|H_{BB}(f)\right|^2.df$

where $H_{BB}(f)$ is the base-band equivalent filter of the front-end filter and Δf_{assym} is the frequency offset between the GNSS carrier frequency and the center of the front-end passband. For instance on E5b, given the proposed filtering requirements by EUROCAE, $\Delta f_{assym}=3\ MHz$ whereas on E5a/L5 $\Delta f_{assym}=0\ MHz$. β is the thermal noise power reduction at correlator output due to front-end filtering. Correlation losses are defined as the loss of SNR at correlator output due to front-end filtering so they equate α/β.

2. **The second term corresponds to the thermal noise and DME/TACAN signal cross-correlation. It is null since signals are independent and zero-mean.**

3. **The last term is the DME/TACAN signal contribution that is computed in the subsequent section.**

DME/TACAN signal characteristics (peak power, central frequency and PRF) determine the blanker duty cycle as well as the noise power increase at correlator output. High-level pulses, pulses whose peak power is larger than the blanking threshold, determine the blanker duty cycle. They also contribute to the noise power increase since some samples are not blanked thanks to the carrier amplitude variations.

Low-level pulses are assumed to not affect the Bdc computation; this hypothesis was verified through simulations. Indeed, low-level pulses constructive combinations causing blanker activation are very unlikely because of carrier phase offsets. Since they are not blanked, all these pulses add noise at the correlator output.

DME/TACAN SIGNAL CONTRIBUTION TO THE NOISE FLOOR

Pulses whose peak power is below the blanking threshold will entirely enter the digital correlator. A convenient way to take into account their effect is to compute the interference coefficient. So as to compute this coefficient, DME/TACAN signal power spectral density is required, so first its autocorrelation function is calculated. To simplify computation, the main assumption in the following is to consider a Gaussian-shape pulse as rectangle, see next plot, whose length T_{eq} is called the equivalent duration of a pulse and is defined as [12]

$$T_{eq}=\frac{1}{J}.\int_{-\infty}^{+\infty}e^{-\alpha t^2}.dt$$

For DME/TACANs $T_{eq}=2.64\ \mu s$. The amplitude A of the rectangle is simply the DME/TACAN square-root peak power.

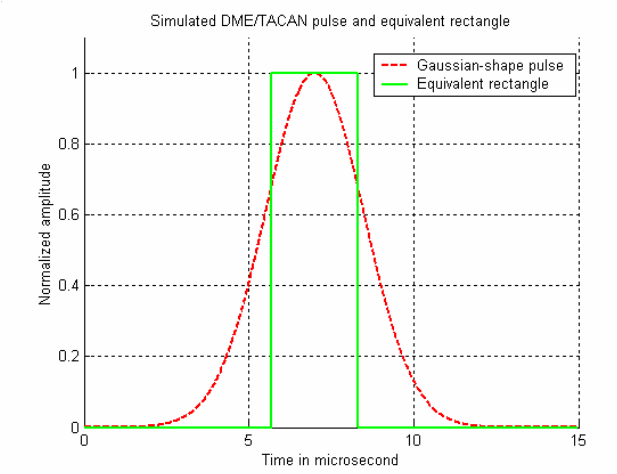

Figure 7 *Simulated DME/TACAN pulse and equivalent rectangle*

It can be shown that the theoretical expression of a DME/TACAN signal autocorrelation function $K_S(\tau)$ is [13]:

$$K_S(\tau)=2K(\tau)+K(\tau-\Delta t)+K(\tau+\Delta t)$$

where $K(\tau)$ is the autocorrelation if single pulses are considered instead of pairs. Assume rectangular-shape pulses, the autocorrelation function is then, [13]:

$$K(\tau) = A^2\left(1 - e^{-\lambda T_{eq}}\right)^2 + m(\tau)$$

with

$$m(\tau) = A^2\left(1 - e^{-\lambda(T_{eq}-|\tau|)} + \left(1 - e^{-|\tau|}\right)^2 - \left(1 - e^{-\lambda T_{eq}}\right)^2\right).I_{[-T_{eq},T_{eq}]}(\tau)$$

and where $I_{[-T,T]}(\tau) = \begin{cases} 1 & if \quad \tau \in [-T,T] \\ 0 & elsewhere \end{cases}$

This theoretical derivation was verified by simulation, next plot presents the theoretical as well as the simulated rectangular-shape and Gaussian-shape autocorrelations of a single DME signal.

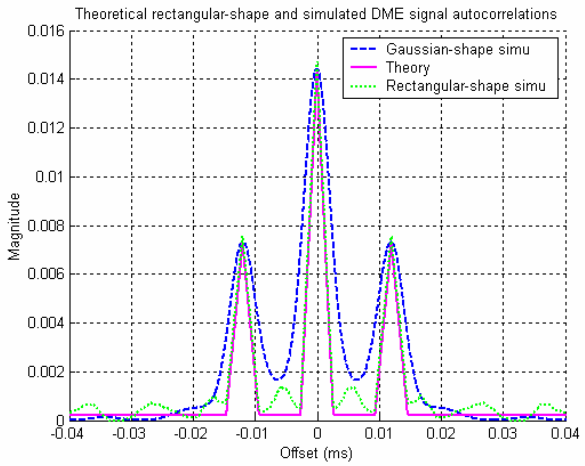

Figure 8 *Gaussian-shape and rectangular-shape simulated and theoretical DME signal autocorrelation*

Theoretical expression matches well simulated signal autocorrelation. We have shown that TACAN autocorrelation is very close to that and so is considered identical. The base-band PSD $S_{jammer,BB}(f)$ of a DME/TACAN signal is then the Fourier transform of this autocorrelation function. A close-up of the obtained theoretical normalized PSD is plotted on Figure 9.

A sinc^2-shape, with nulls every 380 kHz, is easily observed on the PSD plot. It originates from rectangular-shape pulse with length 2.64 µs considered in the theoretical derivation. Moreover, the 12 µs separation between the two pulses of each pair implies smaller internal lobes separated by about 83 kHz.

The interference coefficient $C_I(\Delta f)$ at the frequency offset Δf is defined as [4],

$$C_I(\Delta f) = \int_{-\infty}^{+\infty} |H_{BB}(f)|^2 . S_{jammer,BB}(f - \Delta f) . S_C(f - \Delta f_{assym}) . df$$

where

- $S_{jammer,BB}(f)$ is the base-band normalized DME/TACAN PSD
- $S_c(f)$ is the base-band normalized PSD of the PRN code with chip rate f_c and chip duration $T_c = 1/f_c$
- Δf_{assym} is the frequency offset brought by asymmetric filtering on E5b

We can assume a continuous spreading code PSD neglecting spectrum lines:

$$S_C(f) = \frac{1}{f_c} . \left(\frac{\sin(\pi f T_c)}{\pi f T_c}\right)^2$$

DME and TACAN interference coefficients can be considered equal. Figure 10 shows interference coefficients as a function of the frequency offset on E5a/L5 (symmetric filtering) and on E5b (assymmetric filtering). Because summation is over a larger frequency band on E5a/L5, the associated interference coefficient is larger.

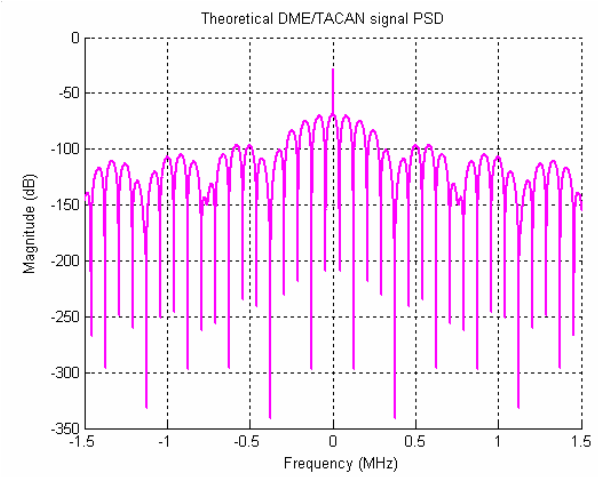

Figure 9 *Close-up of the theoretical normalized DME/TACAN signal PSD*

The corresponding correlator output power P_{out} is then very well approximated by,

$$P_{out} = G_{AGC}^2 . P_{jammer} . C_I(\Delta f) . \frac{f_p}{4}$$

P_{jammer} is the mean DME/TACAN signal power after front-end filtering. According to the Poisson distribution properties, it can be easily demonstrated that

$$P_{jammer} = \frac{J}{2} . |H(f_J)|^2 . (2\lambda T_{eq}) e^{-2\lambda T_{eq}}$$

Note: division by two comes from the carrier effect.

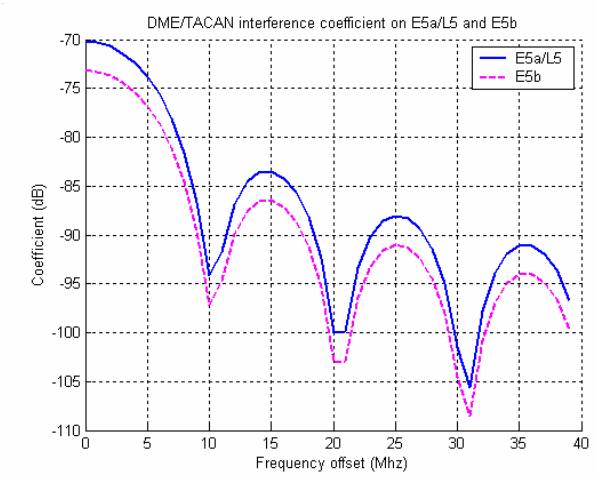

Figure 10 *E5a/L5 and E5b DME/TACAN interference coefficient as a function of frequency offset*

Moreover, because of the pulse blanking system, a portion of the low-level pulse samples will be zeroed so the real power at correlator output must be reduced by the factor *(1-Bdc)* as we did with the receiver thermal noise so finally, for a single DME/TACAN signal

$$P_{out} = G_{AGC}^2 . P_{jammer} . C_I(\Delta f) . \frac{f_p}{4} . (1 - Bdc)$$

Note: Until now, only low-level pulses were considered. Regarding high-level pulses, induced degradations are assumed to equate degradation caused by low-level pulses with instantaneous power equating the blanking threshold. We did this approximation to simplify the derivation. Simulations have shown this approximation was pretty good.

Eventually, the correlator output SNIR in presence of DME/TACAN signals (referenced by index *i*) is:

$$SNIR = \frac{\alpha . \frac{P_{GNSS}}{4} . (1 - Bdc)^2}{\beta . \frac{N_O . f_P}{4} . (1 - Bdc) + \frac{(1 - Bdc) . f_p}{4} . \sum_i P_{jammer,i} . C_{I,i}(\Delta f)}$$

and the equivalent post-correlation C/N_0 degradation (equal to the SNR degradation) with respect to the nominal case (front-end filtering but no interference) is

$$\deg\left(\frac{C}{N_0}_{equ}\right) = \frac{1 - Bdc}{1 + \frac{\sum_i P_{jammer,i} . C_I(\Delta f_i)}{\beta . N_O}}$$

This degradation is not the pure degradation brought by DME/TACAN signals since front-end filtering effect appears through β. However this expression is useful when calculating the power link budget where correlation losses are accounted for first then are DME/TACAN's degradations.

Bdc COMPUTATION

Consider a single strong DME/TACAN pulse: a portion of its samples is larger than the blanking threshold and so is zeroed. The objective is to find this proportion when collisions with other pulses occur and when it modulates a carrier. First assume the absence of the carrier, then given the DME/TACAN peak power at the blanker level $J.|H(f)|^2$ and the digital pulse blanking threshold *Th*, the portion of time *T* when the blanker will be "active" without any pulse superposition is

$$T = 2\sqrt{\frac{\ln\left(\frac{J.|H(f)|^2}{Th}\right)}{\alpha}}$$

Now any additional strong pulses, transmitted by other ground beacons that would occur during this period would decrease the blanker activation time of the initial pulse. The mean value of the activation time T_{mean} when pulse collisions are assumed may be computed from the mean activation times in the absence of collisions $T_{mean/0}$ and in presence of one $T_{mean/1}$, two $T_{mean/2}$ etc…collisions:

$$T_{mean} = T_{mean/0} . P(0\ collision) + T_{mean/1} . P(1\ collision) + T_{mean/2} . P(2\ collisions) + \ldots$$

According to the Poisson distribution properties, the probability $P(N,\tau)$ of having *N* arrival times during τ seconds is [14]

$$P(N,\tau) = \frac{(\lambda.\tau)^N}{N!} . e^{-(\lambda.\tau)}$$

Moreover, one very useful property of such random distributions is that knowing there is one (or more) arrival time(s) during a certain interval of time τ, this arrival time(s) is(are) uniformly distributed over τ. For the sake of simplicity, assume pulses that may enter in collision have blanker activation times at least equal to the blanker activation time of the initial pulse. In reality durations may be shorter if for instance their peak powers are lower. Thus, without any collision,

$$\overline{T}_{/0\ collision} = T$$

for one collision,

$$\overline{T}_{/1\ collision} = \int_0^T t . \frac{1}{T} . dt = \frac{T}{2}$$

for two collisions,

$$\begin{aligned}\overline{T}_{/2\,collision} &= \int_0^T\int_0^T \min(t_2,t_2).p(t_1,t_2)dt_1dt_2 \\ &= \frac{1}{T^2}\left(\int_0^T\int_0^{t_2} t_1.dt_1dt_2 + \int_0^T\int_{t_2}^T t_2.dt_1dt_2\right) \\ &= \frac{1}{T^2}\left(\frac{T^3}{6}+\frac{T^3}{2}-\frac{T^3}{3}\right) \\ &= \frac{T}{3}\end{aligned}$$

and so on…

Eventually, the generic expression of the mean activation time of a strong pulse is (higher order terms are negligible)

$$T_{mean} = T.e^{-\lambda T} + \frac{T}{2}.\frac{(\lambda T)}{1!}.e^{-\lambda T} + \frac{T}{3}.\frac{(\lambda T)^2}{2!}.e^{-\lambda T} + \ldots$$

Note: Parameter λ corresponds, in this case, to the total parameter. For instance, if there are n_{DME} DMEs (PRF=2700) and n_{TACAN} TACANs (PRF=3600), these signals are of course independent then the total parameter is $\lambda=2700*n_{DME}+3600.n_{TACAN}$.

However, because of the carrier variations over the pulse duration, some samples present in the previously defined mean activation time are in fact below the blanking threshold and so are not zeroed. It is illustrated in the next plot for a threshold of 0.6.

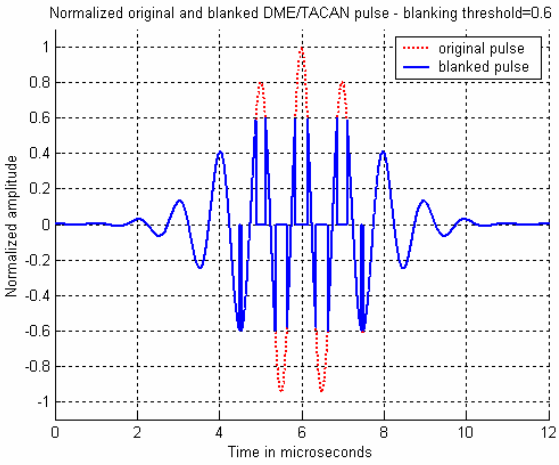

Figure 11 *Original DME/TACAN pulse and the blanked version*

Samples falling below the blanking threshold shouldn't be neglected because they participate to the noise floor at correlator output. Their effect has been described previously.

Thus the real mean activation time is lower; we need to know the number of samples, with time indexes {k}, satisfying:

$$\sqrt{J.|H(f)|^2}.e^{-\alpha\frac{kT_S}{2}}.\cos(2\pi f_0 kT_s + \theta_J) > \sqrt{Th}$$

or equivalently,

$$e^{-\alpha\frac{kT_S}{2}}.\cos(2\pi f_0 kT_s + \theta_J) > \sqrt{\frac{Th}{J.|H(f)|^2}}$$

We remind carrier phase θ_J is unknown and assumed uniformly distributed over [0,2π[. Thanks to simulations, it has been shown that the proportion of samples above the threshold is independent of θ and f_0. So finally, it only depends on the square-root of the blanking threshold to interference peak power (at filter output) ratio. Next plot gives the ratio γ, obtained by simulations, of the real mean activation time to the previously defined mean activation time as a function of $(J.|H(f)|^2)/Th$.

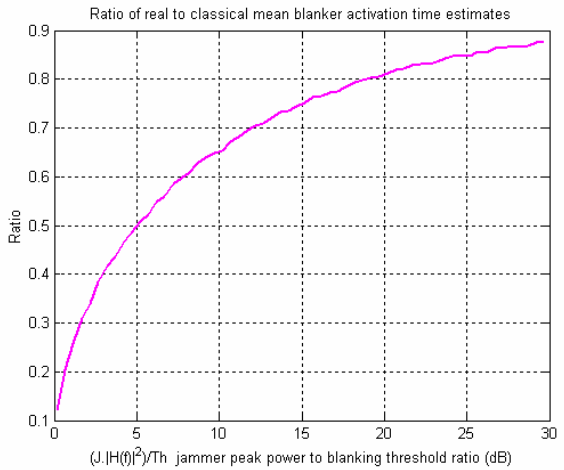

Figure 12 *Ratio of the real activation time of a single pulse to the activation time when assuming pulse envelope only and collisions*

The larger is the power ratio the closer is the real mean blanker activation time to the mean value computed in the absence of carrier. This result may be better understood when considering the probability density function of a sinusoidal function with uniformly distributed phase over [0,2π[, see Figure 13. Clearly there are more samples of the carrier located around extremities than at lower values. So when the ratio $(J.|H(f)|^2)/Th$ is large, the probability for the carrier samples to be above the threshold gets larger as compared with a lower ratio. Thus the real activation time gets closer to the activation time value assuming pulse envelope only. Eventually, the real mean activation time $T_{blanker}$ of a DME/TACAN pulse assuming pulse collision and carrier effect is

$$T_{blanker} = \gamma\left(\frac{J.|H(f)|^2}{Th}\right).\left(Te^{-\lambda T} + \frac{T}{2}\frac{(\lambda T)}{1!}e^{-\lambda T} + \frac{T}{3}\frac{(\lambda T)^2}{2!}e^{-\lambda T} + \ldots\right)$$

Thus the real mean activation time for a set of n_{DME} DMEs (PRF=2700) and n_{TACAN} TACANs (PRF=3600) is

$$T_{blanker,tot} = 2.\left(2700.\sum_{i=1}^{n_{DME}} T_{blanker,DME}(i) + 3600.\sum_{i=1}^{n_{TACAN}} T_{blanker,TACAN}(i) \right)$$

This duration equates the total blanker duty cycle of the DME/TACAN set because it is computed over 1 s.

Note: in the previous expression, factor 2 is due to the presence of pulse pairs instead of single pulses.

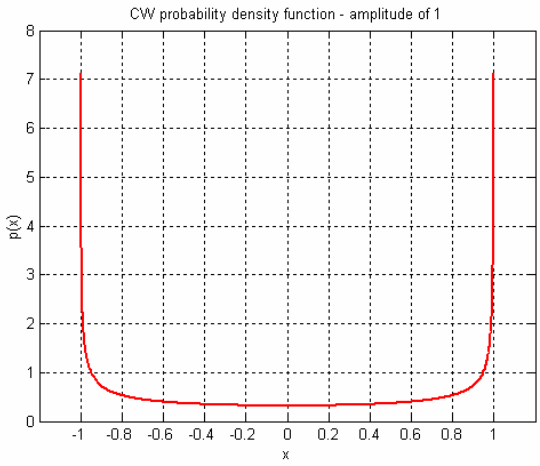

Figure 13 *Unity-amplitude sinusoidal signal probability density function.*

SIMULATOR DESCRIPTION

A complete GLS L5 receiver simulator is available for our tests [15]. This simulator is based on a previously built GPS L1 C/A receiver and has been validated through extensive tests. Because GPS L5 and GALILEO E5a signals will have the same signal structure, computed degradations are assumed identical for these two signals. GALILEO E5b structure is also identical so the only difference when simulating degradation is the equivalent RF/IF front-end filter.
The aim of these simulations is to estimate the equivalent post-correlation C/N_0 degradation and blanker duty cycle due to DME/TACAN signals only. Thus, some functions, such as AGC/ADC system, are not implemented to not take into account associated losses. Only the following functions were used:

- Signals generation: useful GNSS signals, receiver thermal noise, DME/TACAN signals
- Front-end: equivalent RF/IF signal filtering, equivalent digital pulse blanking without AGC/ADC
- Tracking loops: phase lock loop (PLL) and delay lock loop (DLL)

Note: even if there is no AGC/ADC system, digital pulse blanking can be performed equivalently on the simulated "analog" signal. The "analog" signal in the receiver is represented on 64 bits.

Signals are generated according to expressions presented earlier in the paper. Equivalent RF/IF front-end filters implemented in the simulator have frequency responses indicated in Figure 2 and Figure 3.

The opinion of several US experts is that there is no reason to use the data channel for both code and carrier tracking [16]. Indeed most users, such as civil aviation, only care about at which C/N_0 carrier cycle slip occurs. Moreover, even if code tracking is more accurate using both components, tracking errors due to noise are much smaller than other (e.g., multipaths) errors. The achievable improved accuracy does not worth the extra complexity. Thus, the selected tracking configuration in our simulator is to use only the pilot component and the following loop parameters were selected according to results presented in [17]. Carrier phase tracking is performed using a pure PLL (Q discriminator) with 10 ms integration time and a 10 Hz equivalent loop noise bandwidth. Code tracking uses an Early-Minus-Late Power discriminator with 10 ms coherent integration time, 1.5 Hz equivalent loop noise bandwidth and 0.5 chips Early/Late chip spacing. Moreover, loop filters design is based on [18].

THEORETICAL AND SIMULATION RESULTS

Degradations are now computed for the set of DME/TACAN beacons "visible" from an aircraft flying over the worst European location (longitude of 9° and latitude of 50°) at high altitude (FL 400). Only DME/TACANs within the direct line of sight visibility have been considered. The tropospheric refraction effects which may be assessed through a longer 4/3 earth radius radio horizon has not been considered at this stage.

Given the aircraft elevation with respect to each beacon, the proper DME/TACAN beacon antenna gain G_{beacon} is applied to the transmitted power P_{beacon}. We assumed two different antenna gains, plotted in Figure 14, for DME and TACAN beacons. An elevation angle of 0 degrees corresponds to the horizontal direction. It is interesting to note over the European hot spot, the angle of arrival of DME/TACAN signals is always comprised between -20° and 0° at the aircraft antenna level.

Cable loss L_{cable} between the transmitter and the antenna and free space propagation losses L_{free} are accounted for. Moreover regarding the aircraft antenna gain G_{air}, *it* is assumed constant (-10 dBi) for elevations from -30° to -

90° degrees. From 0° to -30°, as proposed by RTCA SC-159 WG 6, it corresponds to a line joining -6 dBi and -10 dBi.

DME/TACAN signal polarization is vertical and so is different from the RHCP polarization of GNSS signals. However, according to [19] we can assume aircraft-installed GNSS antenna have a 0 dB polarization mismatch loss for vertical polarization signals over the lower hemisphere. Eventually, interference power, in dB, at the antenna port is $J=P_{beacon}+L_{cable}+G_{beacon}+L_{free}+G_{air}$.

Correlation losses α/β due to front-end filtering are included in the SNIR estimate obtained from simulation data so they must be subtracted. These losses were estimated by simulation and are respectively -0.43 dB and -0.42 for the simulated EUROCAE and RTCA filters and 0.92 dB for the simulated E5b filter.

A higher receiver noise figure of 5 dB for E5a/L5 and E5b than for L1 has been widely accepted. The reason is the expected larger filter insertion loss due to more stringent filtering requirements. With a 100 °K sky noise, the resulting thermal noise power spectral density is N_0= *-200 dBW/Hz*. This figure is considered for the two tools.

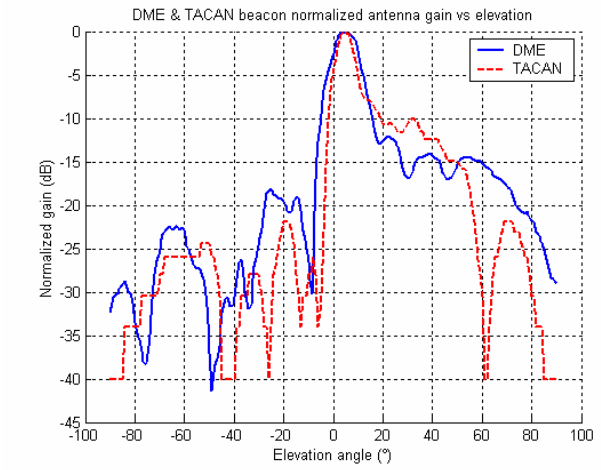

Figure 14 *Considered DME/TACAN beacon antenna gains versus elevation*

Simulations have shown negligible differences in degradations and blanker duty cycles for the two proposed masks (RTCA and EUROCAE) so no distinction will be made in the following.

Next tables present the Bdc and equivalent post-correlation C/N_0 degradation estimates obtained by the theoretical derivation and simulations. A safety margin of either 3 dB or 6 dB was also applied to the transmitted power by DME/TACAN beacons. Four blanking thresholds were considered on E5a/L5: -120.0, -118.4 dBW, -117.1 and -115.9 dBW and the following results were obtained:

blanking threshold (dBW)	***-120.0*** *simu/theory*	***-118.4*** *simu/theory*	***-117.1*** *simu/theory*	***-115.9*** *simu/theory*
0 dB margin				
degradation (dB)	-8.0/-7.4	-7.5/-7.5	-7.9/-7.8	-8.2/-8.2
Bdc	0.40/0.40	0.34/0.33	0.29/0.28	0.26/0.24
3 dB margin				
degradation (dB)	-9.5/-9.3	-9.7/-9.4	-9.5/-9.6	-9.4/-9.8
Bdc	0.48/0.53	0.43/0.45	0.38/0.40	0.34/0.35
6 dB margin				
degradation (dB)	-10.6/-11.6	-10.3/-11.4	-10.4/-11.5	-10.9/-11.8
Bdc	0.56/0.65	0.52/0.59	0.48/0.53	0.44/0.48

Table 1 *Simulated and theoretical results obtained for the E5a/L5 band*

Now on E5b, simulations and theoretical derivation have led to the following results with four blanking thresholds (-121.9, -120.0, -118.4 and -117.1 dBW):

Blanking threshold (dBW)	***-121.9*** *simu/theory*	***-120.0*** *simu/theory*	***-118.4*** *simu/theory*	***-117.1*** *simu/theory*
0 dB margin				
degradation (dB)	-5.5/-4.6	-5.4/-5.2	-6.0/-5.8	-6.3/-6.3
Bdc	0.34/0.33	0.27/0.28	0.23/0.23	0.20/0.20
3 dB margin				
degradation (dB)	-5.8/-5.1	-5.6/-5.7	-6.4/-6.4	-6.8/-7.0
Bdc	0.39/0.41	0.34/0.36	0.30/0.32	0.27/0.28
6 dB margin				
degradation (dB)	-6.6/-5.7	-6.5/-6.3	-6.7/-6.9	-7.3/-7.6
Bdc	0.45/0.49	0.40/0.44	0.36/0.40	0.33/0.36

Table 2 *Simulated and theoretical results obtained for the E5b band*

Clearly there is a great agreement between the blanker duty cycles and equivalent post-correlation C/N_0 degradations computed from the developed theory and simulations. Less accurate theoretical results are obtained when implementing a 6 dB safety margin on E5a/L5. Simulations results are, of course, more trustworthy. Except the 6 dB-margin case on E5a/L5, estimation errors of simulation results by the developed theory are always lower than 1 dB on degradation and lower than 0.04 on the Bdc.

An important result is that degradation is lower on E5b by about 2 dB without safety margin. With a safety margin of 6 dB, E5b degradation is even lower by about 3.5 dB. Finally, a safety margin of 6 dB yields much higher degradations on both bands; there is an increase of about 2.5 dB on E5a/L5 and about 1 dB on E5b.

GEOGRAPHICAL DEGRADATION MAPS OVER EUROPE

Theoretical derivation of the equivalent post-correlation C/N_0 degradation and blanker duty cycle has been validated through tests using the GNSS receiver simulator. So we can compute theoretical degradations over the whole of Europe at FL 400. Figure 15 shows the

DME/TACAN beacon locations (circles on the figure) in Europe that reply in the 1151-1213 MHz band (X-mode).

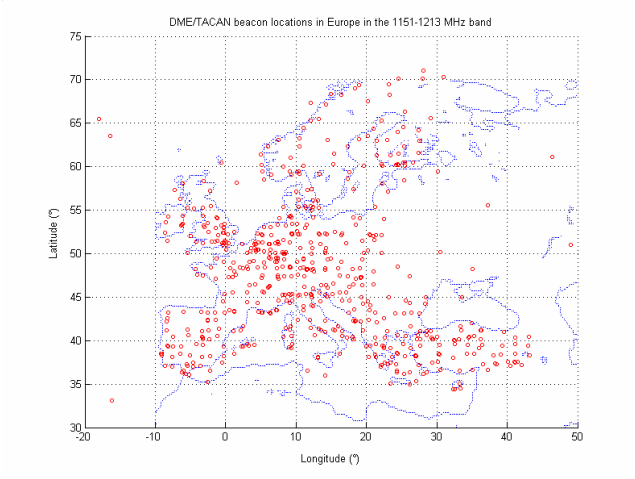

Figure 15 *Locations of DME/TACAN beacons in Europe replying in the 1151-1213 MHz band (X mode)*

Here is the E5a/L5 degradation plot over Europe for a blanking threshold of -118.4 dBW:

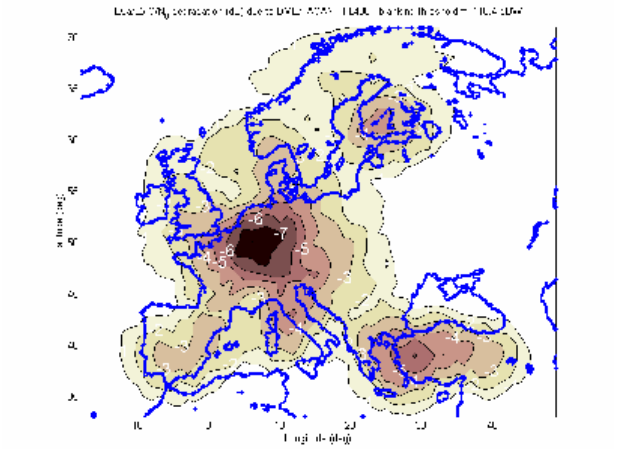

Figure 16 *Theoretical E5a/L5 degradation over Europe due to DME/TACAN signals – blanking threshold -118.4 dBW*

On E5b we get the results indicated on Figure 17 with a blanking threshold of -120 dBW. The European hot-spot location is obvious on the two previous plots.

BLANLKING THRESHOLD OPTIMIZATION

Up to now, only four blanking thresholds were considered on each band leading to different results. Thus simulations were run on both bands for multiple thresholds to estimate the optimal blanking threshold with respect to Bdc and equivalent post-correlation C/N_0 degradation. We used simulations instead of the theoretical derivation since the former are more trustworthy. Figure 18 presents results for E5a/L5.

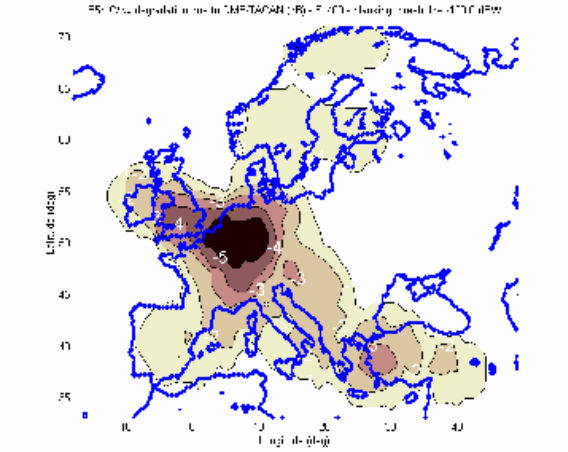

Figure 17 *Theoretical E5b degradation over Europe due to DME/TACAN signals – blanking threshold -120.0 dBW*

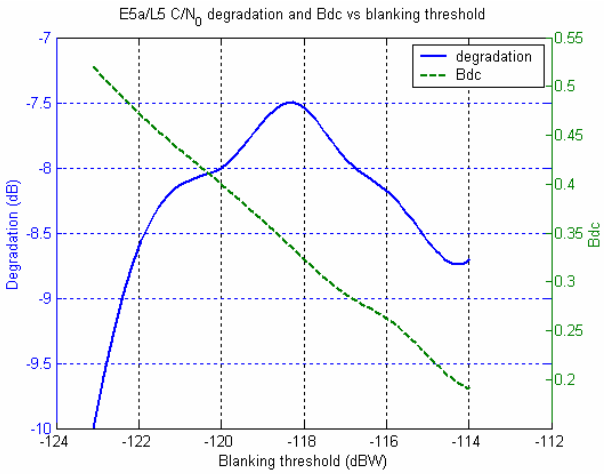

Figure 18 *Simulated E5a/L5 C/N_0 degradation and Bdc versus blanking threshold over the European hot-spot*

Thus E5a/L5 degradation is pretty constant: from 7.5 dB to 8.5 dB if the blanking threshold is comprised between -122 dBW and -115 dBW. However the Bdc varies greatly: from 0.22 to 0.45. On E5b we get the results shown in Figure 19. Again, the degradation is pretty constant: from 5.4 dB to 6.0 dB if the blanking threshold is comprised between -123.5 dBW and -118.5 dBW. However the Bdc varies largely: from 0.22 to 0.38. The four previously selected thresholds for each band are around the optimal blanking threshold.

REASSIGNMENT OF DME/TACAN BEACONS

One suggested way to reduce degradation is to reassign DME/TACAN beacons transmitting around E5a/L5 and

E5b. Thus theoretical equivalent post-correlation C/N_0 degradation and blanker duty cycle are computed in this section as a function of the bilateral reallocation bandwidth over the European hot-spot at FL 400. For instance a bilateral reallocation of 2 MHz on E5a corresponds to the exclusion of all DME/TACAN beacons transmitting in *[E5a-1MHz,E5a+1MHz]*. Figure 20 shows results on E5a/L5 when the blanking threshold equates -118.4 dBW.

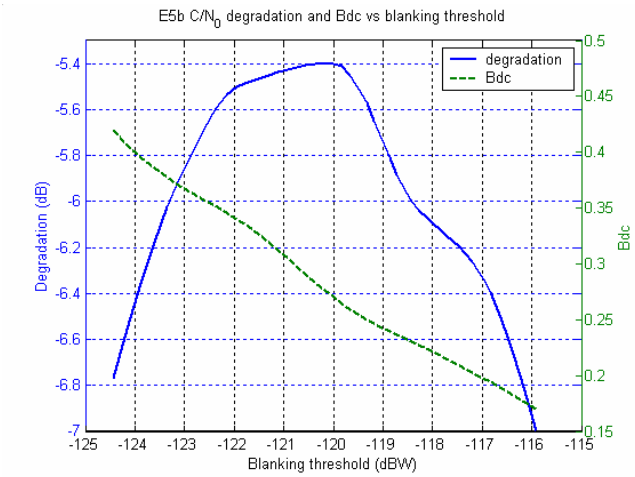

Figure 19 Simulated E5b C/N_0 degradation and Bdc versus blanking threshold over the European hot-spot

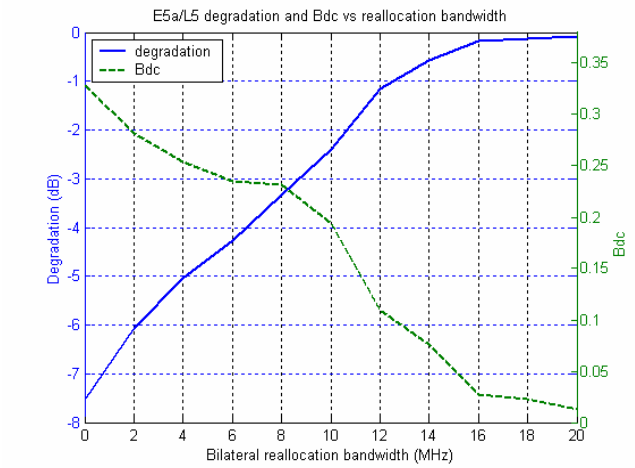

Figure 20 Theoretical E5a/L5 C/N_0 degradation and Bdc as a function of the bilateral reallocation bandwidth over the European hot-spot

Degradation could be reduced by a factor 2 if all the beacons transmitting within +/- 5 MHz around E5a/L5 are reallocated. On E5b, with a blanking threshold of -120 dBW we get results of Figure 21. In this band a bilateral reallocation of 10 MHz almost cancel degradations.

CONCLUSION

In this paper we proposed two approaches to assess the impact of DME/TACAN signals that are the main threat for the future GALILEO E5a/E5b and GPS L5 signals. The theoretical approach enables to better understand what will happen in future receivers because of these pulsed signals. Thanks to it reliable results can be obtained very quickly. The simulation tool requires longer running times but more confidence can be placed in the obtained numbers. Thus these two tools are complementary.

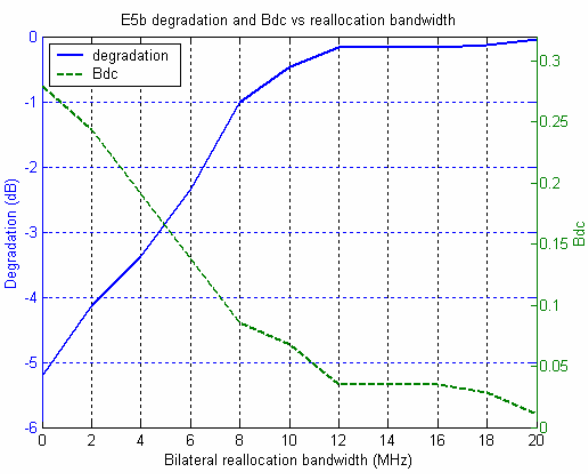

Figure 21 Theoretical E5b C/N_0 degradation and Bdc as a function of the bilateral reallocation bandwidth over the European hot-spot

Obtained results are very useful to assess the performance of receiver functions using prompt correlator output samples such as signal acquisition and phase tracking. One application is the establishment of power link budgets to evaluate the usability of navigation signals at high altitude. We have found at FL 400 with an adapted blanking threshold the minimum degradation is about 7.5 dB on E5a/L5 while on E5b it is about 5.5 dB.

With a 6 dB safety margin, degradations are much larger: about 10.5 dB on E5a/L5 and about 6.5 dB on E5b.

Reallocation of DME/TACAN beacons seems to be an efficient way to reduce the impact of DME/TACAN signals on GNSS receivers. However this solution is expensive.

REFERENCES

[1] Hegarty, C., T. Kim, S. Ericson, P. Reddan, T. Morrissey, and A.J. Van Dierendonck, *"Methodology for Determining Compatibility of GPS L5 with Existing Systems and Preliminary Results"*, Proceeding of the Institute of Navigation Annual Meeting, Cambridge, MA, June 1999

[2] M.Tran and al., *"Validation of the feasibility of coexistence of the new civil GPS signal (L5) with existing systems"*, MITRE paper, February 2001

[3] Y.Ernou, *"E5 band RF Interference Environment and receivers susceptibility"*, 6th EUROCAE meeting, working paper 12, Madrid, 8-9 April 2003

[4] A.J. Van Dierendonck, *"GPS receivers"*, Global Positioning System: Theory and Application, B.Parkinson and J.J Spilker, JR., Ed ., Washington, D.C.: AIAA, Inc., 1996

[5] H.Chang, *"Presmapling, Filtering, Sampling and Quantization Effects on the Digital Matched Filter Performance"*, Proceedings of the International Telemetering Conference, 1982, pp. 889-915

[6] Grabowski, J, Hegarty, C, *"Characterization of L5 Receiver Performance Using Digital Pulse blanking"*, Proceeding of The Institute of Navigation GPS Meeting, Portland, OR, September 2002

[7] A.J Van Dierendonck, J.J Silker Jr, *"Proposed New Civil GPS signal at 1176.45 MHz"*, Proceedings of the Institute of Navigation GPS meeting, Salt Lake City, Utah, September 1999

[8] GALILEO Signal Task Force, *"Status of GALILEO Frequency and Signal Design"*, Proceedings of the Institute of Navigation GPS meeting, Salt Lake City, Utah, September 1999

[9] Monnerat, M, Lobert, B, Journo, S, Bourga, C, *"Innovative GNSS2 navigation Signal"*, Proceedings of The Institute of Navigation GPS Meeting, Salt Lake City, Utah, September 2001

[10] J.W Betz, *"Effect of Narrowband Interference on GPS Code Tracking Accuracy"*, Proceedings of The Institute of Navigation NTM Meeting, Anaheim, CA, January 2000

[11] F.Bastide, *"Correlation losses expressions"*, ENAC/STNA working note, November 2003

[12] C.Hegarty, *"Pulse Width for L5 Compatibility"*, MITRE working note, May 11, 1999

[13] F.Bastide, J.Y Tourneret, *"DME/TACAN signal autocorrelation computation"*, ENAC/STNA/TeSA working note, September 2003

[14] J.P Delmas, *"Probabilités et Télécommunications"*, Mason, 1987

[15] F.Bastide et al., *"Assessment of L5 Receiver Performance in presence of Interference using a Realistic Receiver Simulator"*, Proceedings of The Institute of Navigation GPS Meeting, Portland, OR, September 2003.

[16] Personnal conversation with Chris Hegarty, August 2003

[17] M.Tran, C.Hegarty**,** *"Performance Evaluations of the New GPS L5 and L2 Civil (L2C) Signals"*, Proceedings of the Institute of Navigation National Technical Meeting, Anaheim, CA, January 2003

[18] Stephens, S.A., and J.C. Thomas, *"Controlled-Root Formulation for Digital Phase-Locked Loops"*, IEEE Transactions on Aerospace and Electronic Systems, January 1995

[19] Anon, *"Assessment of Radio Frequency Interference Relevant to the GPS – appendix G"*, RTCA, January 1997